Journal of Alloys and Compounds 731 (2018) 914–919

Contents lists available at ScienceDirect

Journal of Alloys and Compounds

journal homepage: http://www.elsevier.com/locate/jalcom

Fe^{3+}/Nb^{5+} co-doping effects on the properties of Aurivillius $Bi_4Ti_3O_{12}$ ceramics

C. Lavado, M.G. Stachiotti*

Instituto de Fisica Rosario, Universidad Nacional de Rosario, 27 de Febrero 210 Bis, 2000 Rosario, Argentina

ARTICLE INFO

Article history:
Received 28 July 2017
Accepted 15 October 2017
Available online 16 October 2017

Keywords:
Ferroelectrics
Ceramics
Solid state reaction
Dielectric response

ABSTRACT

$Bi_4Ti_{3-x}(Nb_{0.5}Fe_{0.5})_xO_{12}$ (BTFNx) ceramics with $0 \leq x \leq 2$ were synthesized to evaluate the effect of Fe^{3+}/Nb^{5+} co-substitution into the B-site of $Bi_4Ti_3O_{12}$ (BIT). We show that the XRD pattern for the compounds with $x \leq 1$ is the characteristic one of a layered perovskite structure belonging to the $n = 3$ member of the Aurivillius family. Impurity peaks assigned to a pyrochlore phase are detected at higher concentrations. Raman measurements corroborated that $Fe^{3+}$and Nb^{5+} ions are incorporated into the Ti sites of the Aurivillius compound. Frequency dependent dielectric studies at room-temperature displayed the reduction of both dielectric constant and loss tangent with substitution, while the electric-field-induced polarization switching behavior indicates ferroelectric character. It is observed that the ferroelectric transition temperature decreases with increasing Fe/Nb content. Magnetic measurements indicated no evidence of ferromagnetic ordering, but antiferromagnetic spin correlations between Fe^{3+} ions.

1. Introduction

Bismuth titanate ($Bi_4Ti_3O_{12}$, BIT) is one of the simplest compounds in the Aurivillius family with a vast potential for applications in the electronic industry. It exhibits excellent performance for NvRAMs applications due to their fatigue free nature and other electric properties [1,2]. In addition, when compared to other ferroelectric materials ($BaTiO_3$, $PbZr_xTi_{1-x}O_3$, etc.), this compound exhibits a high Curie temperature, which makes it useful over a wide temperature range [3]. Its crystal structure consists of $(Bi_2O_2)^{2+}$ sheets alternating with $(Bi_2Ti_3O_{10})^{2-}$ perovskite-like layers stacked along the crystallographic c direction. This crystal anisotropy is reflected in the grain growth habit, where a plate-like morphology gives rise to electrical anisotropy. The platelets are apparently single crystals with the c-axis perpendicular to the major face and with the higher component of its spontaneous polarization parallel to this face. The electrical conductivity is also highly anisotropic, with the maximum value in the same plane as the polarization.

In order to improve specific properties of BIT ceramics, solid solutions with other cations have been considered and explored. For instance, it is naturally expected to realize multiferroic properties and magnetoelectric coupling by doping with magnetic ions. Related investigations mainly focused on Fe/Co at the Ti-sites and Nd/Sm/Gd at the Bi-sites [4–9], but problems such as large leakage current, poor ferroelectricity and weak ferromagnetism are encountered. In Fe doped BIT ceramics, for instance, the shape of the hysteresis loops does not correspond to a classical ferroelectric type but is indicative of leakage current in the samples [4,5]. This can be explained by the arising of oxygen vacancies to ensure charge neutrality when the Ti^{4+} ion is substituted for Fe^{3+}. A possible strategy to avoid the generation of oxygen vacancies in Fe doped BIT is the co-doping with +5 ions (for example, Nb^{5+}). In this way the vacancies generated by the addition of iron are suppressed for equimolar compositions of Nb^{5+} and Fe^{3+}. We note that Fe^{3+}/Nb^{5+} (or Fe^{3+}/Ta^{5+}) co-doping of PZT ceramics has been recently proposed as a route to fabricate single-phase room-temperature multiferroic magnetoelectrics [10–13]. In this work we investigate the effect of Fe^{3+}/Nb^{5+} co-substitution on the structural, electric, and magnetic properties of BIT.

2. Experimental procedure

$Bi_4Ti_{3-x}(Nb_{0.5}Fe_{0.5})_xO_{12}$ (BTFNx) ceramics with $0 \leq x \leq 2$ were

* Corresponding author.
E-mail address: stachiotti@ifir-conicet.gov.ar (M.G. Stachiotti).

https://doi.org/10.1016/j.jallcom.2017.10.112
0925-8388/

synthesized by the solid state reaction method. The powders were prepared from a mixture of Bi_2O_3, TiO_2, Fe_2O_3 and Nb_2O_5 by a milling process using a planetary ball mill equipment (Torrey Hills Technologies ND 0.4 L). Raw materials were weighed based on the stoichiometric formula and milled in absolute alcohol for 4 h. Dried powders calcined at 800 °C for 5 h were milled again for 4 h. The obtained powders were mixed with a polyvinyl butyral (PVB) binder solution and then die-pressed into disks with dimensions of Ø10 mm × 2 mm. The discs were sintered at 950 °C for 3 h in air and then cooled at 5 °C/min to room temperature.

Crystal structure was analyzed by X-ray diffraction (XRD) using a Philips X'Pert Pro X-ray diffractometer. Raman spectra were acquired with a Renishaw in Via Raman spectrometer by means of the 514 nm Ar-ion laser line (10 mW nominal power). The microstructure of the samples was examined by Scanning Electron Microscopy (SEM) using a LEITZ AMR 1000. For electrical studies, silver electrodes were coated onto the polished surfaces ceramic samples. The temperature dependence of the dielectric properties of the ceramics was measured using an LCR meter (QuadTech 7600 plus) attached to a programmable furnace. The ferroelectric hysteresis loops were measured at 50 Hz using a Sawyer-Tower circuit. Magnetic measurements as a function of the temperature and applied magnetic field were carried out using aVersaLab™ magnetometer manufactured by Quantum Design, Inc.

3. Results and discussions

Fig. 1 shows the XRD patterns of BTFNx ceramic samples. The peaks are indexed for an orthorhombic system. The spectra show that single phases with a Bi-layered perovskite structure were formed at concentrations $x \leq 1$. No extra peaks related to unreacted (starting oxides and pyrochlore) or other unwanted phases have been observed at those concentrations, indicating the formation of a single phase belonging to the $n = 3$ member of the Aurivillius family. The observed shift of the XRD peak (117) to lower angles indicates an increase in the lattice parameters and the unit cell volume when Fe/Nb concentration increases. We note that the degree of c orientation of the ceramic samples for $x \leq 1$ practically does not depend on the Fe/Nb content. This scenario changes at higher concentrations due to the presence of a secondary phase. The XRD patterns of the samples with $x = 1.5$ and 2.0 reveal the existence of impurity peaks. Clearly, those peaks can be assigned to $Bi_2Ti_2O_7$, a cubic pyrochlore phase that usually accompanies BIT in the Bi_2O_3-TiO_2 reaction system [14]. It is also observed in Fig. 1 that the amount of the unwanted $Bi_2Ti_2O_7$ phase increases considerably when x increases from 1.5 to 2.0.

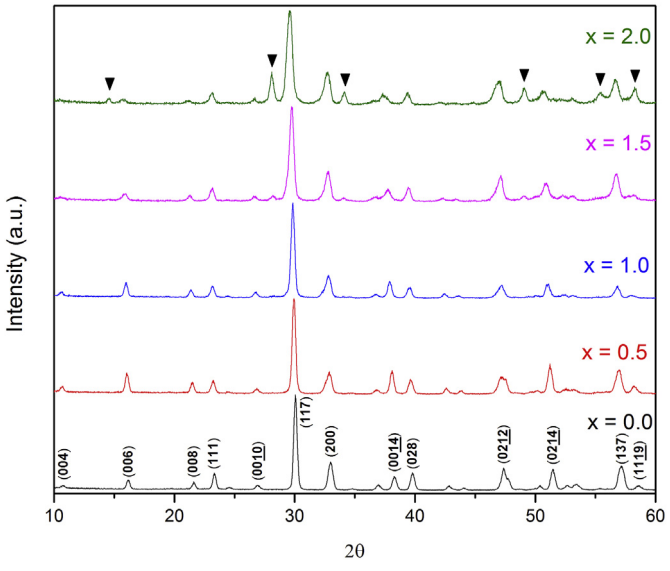

Fig. 1. XRD patterns of BTFNx ($x = 0.0, 0.5, 1.0, 1.5$ and 2.0) ceramics sintered at 950 °C. The peaks are indexed for an orthorhombic system. Black symbols identify peaks corresponding to the pyrochlore phase.

Fig. 2 shows SEM images of BTFNx ceramics with $x = 0$ (a), 0.5 (b), 0.8 (c), 1.0 (d), and 2.0 (e and f). The surface morphology of samples with $x \leq 1$ shows the formation of randomly oriented plate-like grains, which is a characteristic feature of the Aurivillius compounds, indicating that Fe/Nb co-doping does not alter the layered microstructure. It can be noticed that the average grain size decreases with increasing Fe^{3+} and Nb^{5+} content. While platelike grains with sizes of ~10 μm are observed for the BIT pure phase (Fig. 2a), the grains of the doped samples are smaller (~5 μm for $x = 0.5$, and ~3 μm for $x = 0.8$ and $x = 1.0$). A different microstructure is observed at higher Fe/Nb concentrations, where grains with two different morphologies are detected. Fig. 2e shows the presence of grains with polyhedral morphology corresponding to $Bi_2Ti_2O_7$. It is well known that the appearance of the pyrochlore secondary phase in Aurivillius compounds also produces an exaggerated grain growth affecting the material properties. The low magnification image of Fig. 2f indicates that the pyrochlore is the dominant phase at $x = 2.0$. The image also shows the presence of isolated porosity, often observed in $Bi_2Ti_2O_7$ [14]. The elemental composition analysis of the ceramic samples by EDS, as shown in the inset of Fig. 2d and f, confirms that Fe^{3+} and Nb^{5+} ions are well incorporated into the system. The data for the sample $x = 2.0$ were collected on the polyhedral grains, and confirms that Fe^{3+} and Nb^{5+} ions are also incorporated in the pyrochlore phase. This is supported by investigations showing that the pyrochlore is able to host mixed-valence metals, such as Fe and Nb [15,16].

Structural properties at local scale were investigated by Raman spectroscopy analyses. Fig. 3 shows Raman spectra of BTFNx ceramics at room temperature. The spectrum for pure BIT exhibits phonon peaks at 117, 148, 183, 227, 269, 332, 354, 450 537, 563, 611 and 848 cm−1, in agreement with other spectra reported in the literature. Vertical lines are included in the figure to visualize the variation of the most intense phonon peaks with doping. It is clear that the samples with $x \leq 1$ display spectra similar to BIT. The spectrum for $x = 2.0$ was collected on the polyhedral grains.

It is known that in BIT the heavy Bi ions are expected to exhibit their contribution in the lower frequency regime, while modes above 200 cm^{-1} have been assigned as internal modes of TiO_6 octahedra [17]. Therefore, the little variation with doping of the mode at 117 cm^{-1} implies the Bi ions do not participate in the substitution process. In contrast, modes in the broad band between 200 and 400 cm^{-1} became diffuse and their frequency decreased with increasing Fe/Nb content. The shifting in those modes to smaller vibrational frequencies is due to the substitution of the heavier Fe/Nb atoms at Ti-sites. In summary, results obtained from Raman spectra correlate well with the results presented above, and corroborate that the Fe^{3+} and Nb^{5+} ions are incorporated into the Ti sites.

Fig. 4a and b shows the variation of the room-temperature dielectric constant (ε_r) and loss tangent ($\tan\delta$) as a function of frequency. Almost negligible dispersion is observed for all the ceramic samples over the range 1 KHz−1MHz. Both, ε_r and $\tan\delta$ values decrease with Fe/Nb content for $x < 1$. One possible cause is the smaller grain size of the doped samples, as mentioned above. $Bi_4Ti_2Nb_{0.5}Fe_{0.5}O_{12}$, for instance, has a dielectric constant of ~115 (145 for BIT), negligible frequency dispersion and a dissipation factor less than 0.01. The variation of ε_r and $\tan\delta$ with x measured at 100 KHz is displayed in Fig. 4c. The figure shows an increase of the

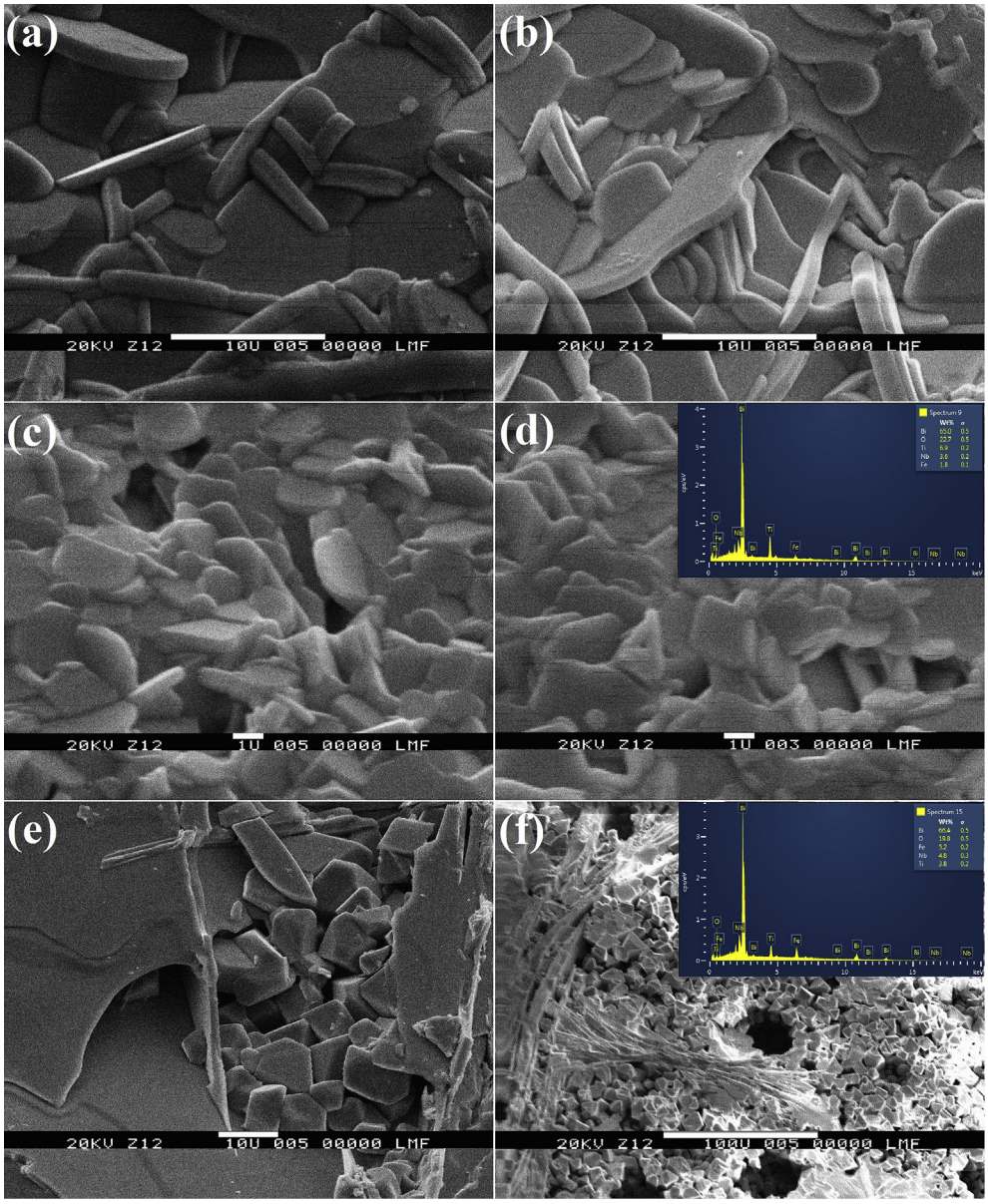

Fig. 2. SEM images showing surface morphologies of BTFNx ceramics with x = 0.0 (a), x = 0.5 (b), x = 0.8 (c), x = 1.0 (d) and x = 2.0 (e and f). The insets show elemental composition analysis by EDS of the ceramic samples with x = 1.0 and x = 2.0.

dielectric constant at high Fe/Nb concentrations. This can be explained the fact the pyrochlore phase gives rise to a material with a relatively high dielectric constant (used as storage capacitors in dynamic random access memory) [18].

Fig. 5a shows the temperature dependence of the dielectric constant. The corresponding losses are plotted in Fig. 5b. The data were taken during the heating process of the thermal cycle. Although we made measurements at different frequencies, only the data for 500 KHz are presented for the sake of clarity. It is observed that the ferroelectric phase transition temperature (T_c) decreases with increasing Fe/Nb content. In particular, the $Bi_4Ti_2Nb_{0.5}Fe_{0.5}O_{12}$ sample displays a transition temperature ~40 °C lower than BIT. This may be attributed to the reduction of orthorhombic distortions in the system with substitution. As it is shown in the inset of Fig. 5a for the case x = 1.0, BTNFx ceramics do not display relaxor-like behavior. However, we note that the ferroelectric peak becomes smaller and wider when Fe/Nb replaces Ti, which may be related to the different grain size. Fig. 5 shows that the sample with x = 2.0 displays a peak at T = 630°C, indicating the presence of the Aurivillius phase together with the dominat pyrochlore phase. We note that the values of ε_r and tanδ remarkably increase with increasing temperature, indicating the presence of thermally activated charges, such as space charges, charged defects, and related defect complexes. The contribution of grains and grain boundaries to dielectric relaxations and conduction in $Bi_4Ti_2Nb_{0.5}Fe_{0.5}O_{12}$ ceramics has been recently investigated [19].

Polarization-electric field (P-E) hysteresis loops of the Fe/Nb co-doped samples are shown in Fig. 6. The measurements were performed at 50 Hz. We observe that the crystal anisotropy of the BIT structure produces a preferential conductance direction along the $(Bi_2O_2)^{2+}$ layer (in the same plane as the polarization), making it difficult to obtain a high polarization in the material. Futhermore, as it well known, the coercive field of BIT is extremely high, and unfortunately it was not possible to apply electric fields higher than

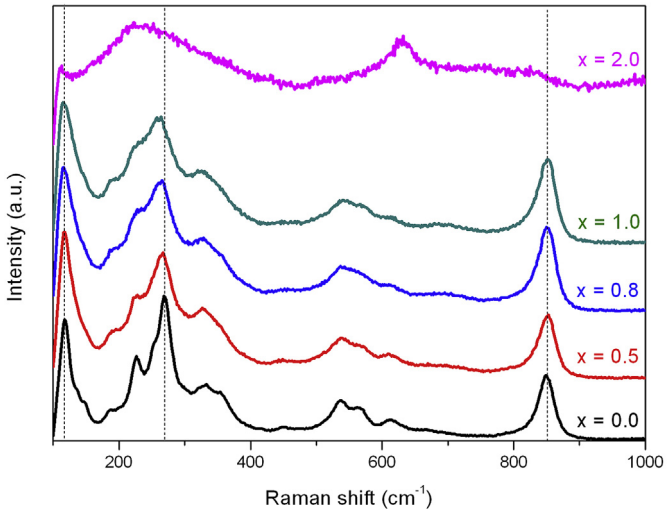

Fig. 3. Raman spectra of BTFNx (x = 0.0, 0.5, 0.8, 1.0, and 2.0) ceramics. Vertical lines are used to visualize the frequency variation of the most intense phonon peaks with doping.

60 kV/cm without producing dielectric rupture. Despite these complications, Fig. 6 shows that the Fe/Nb codoped samples display ferroelectric loops without signatures of high conductivity, indicating ferroelectric character for $x \leq 1$. The switching behavior of the sample with the highest Fe/Nb content ($x = 2.0$) is in concordance with the dielectric nature of the $Bi_2Ti_2O_7$ pyrochlore phase [20].

Fig. 7a shows the field dependences of the magnetization obtained for the samples at room temperature and T = 50 K (for x = 1.0 and 2.0). In contrast to previous investigations suggesting the appearance of a small spontaneous magnetization in Fe doped BIT ceramics [4,5], the Fe/Nb co-doped system revealed paramagnetic behavior. As was mentioned in the introduction, the shape of the ferroelectric hysteresis loops in Fe doped BIT [4,5] is indicative of leakage current in the samples due to the arising of oxygen vacancies. These vacancies could explain the observed room-temperature ferromagnetism by the F-centre exchange mechanism [21,22]. As the Fe/Nb co-doping strategy avoids the generation of oxygen vacancies, a predominant antiferromagnetic interaction between Fe^{3+} moments can be expected for 180° superexchange interactions. We note that ab-initio calculations in $Bi_5FeTi_3O_{15}$ [23] showed a strong antiferromagnetic coupling between Fe^{3+} ions in nearest neighbor positions, characteristic of the superexchange interaction between d^5 cations. We show in Fig. 7b that the magnetic susceptibilities of the samples (χ_m) obey the Curie–Weiss law $\chi_m = C/(T - \theta)$, where C is the Curie constant and θ is the Curie-Weiss temperature. The obtained values of θ are approximately −10.0 K, −30.0 K, and −80.0 K for x = 0.5, 1.0, and 2.0 samples, respectively; thus implying antiferromagnetic spin correlations. The effective magnetic moment (per Fe ion) derived from the corresponding Curie constant of the $Bi_4Ti_2Nb_{0.5}Fe_{0.5}O_{12}$ ceramic sample is $4.91\mu_B$, close to that expected for non-interacting Fe^{3+} ions.

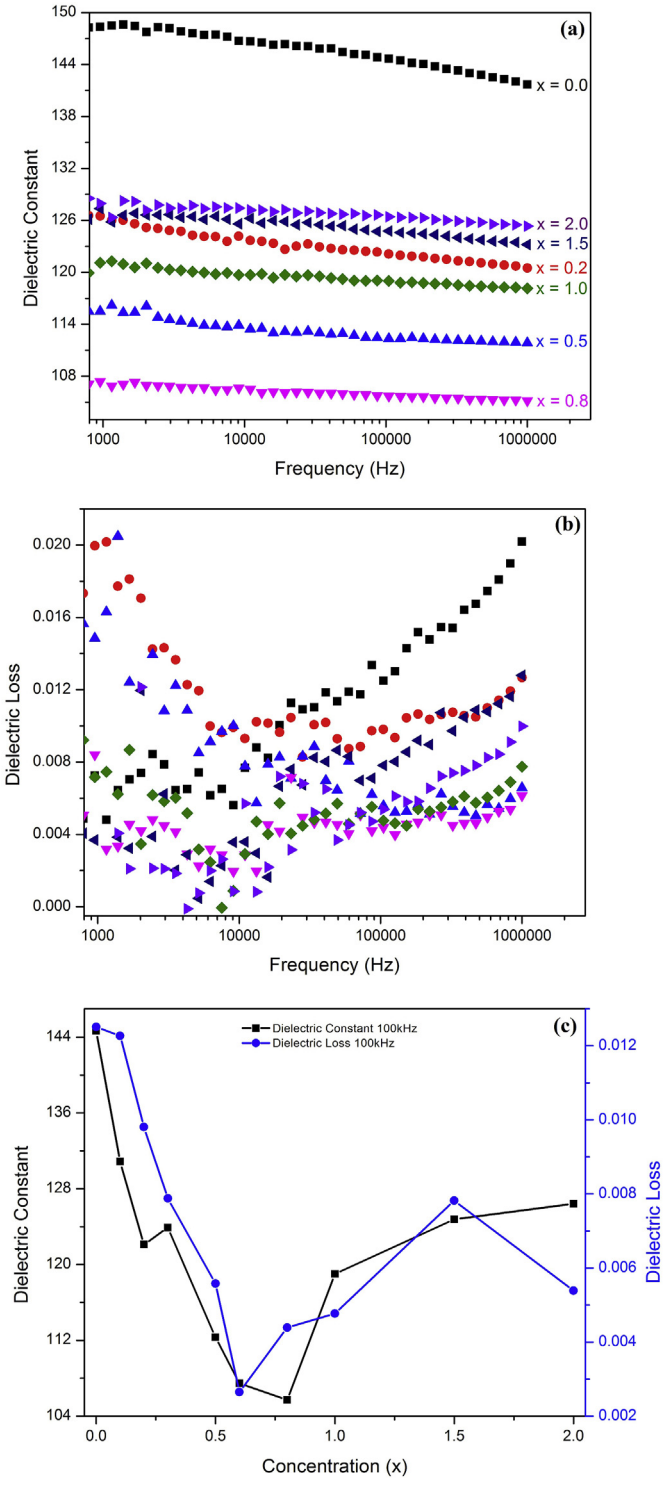

Fig. 4. Room-temperature dielectric constant (a) and loss tangent (b) as a function of frequency. (c) Variation of dielectric constant and loss tangent at 100 KHz with Fe/Nb content.

4. Conclusions

The effect of Fe^{3+}/Nb^{5+} co-substitution into the Ti-site of $Bi_4Ti_3O_{12}$ was investigated. We showed that $Bi_4Ti_{3-x}(Nb_{0.5}Fe_{0.5})_xO_{12}$ ceramics with $x \leq 1$ display the characteristic crystal structure of the n = 3 member of the Aurivillius family. Raman measurements indicated that Fe^{3+} and Nb^{5+} ions are incorporated into the Ti sites of the BIT compound. The dielectric behavior of doped ceramics displayed negligible frequency dispersion and dissipation factor less than 0.01. The ferroelectric transition temperature decreases with increasing Fe/Nb content. Standard Sawyer-Tower measurements indicated ferroelectric character, while magnetic measurements showed antiferromagnetic spin correlations between Fe^{3+}

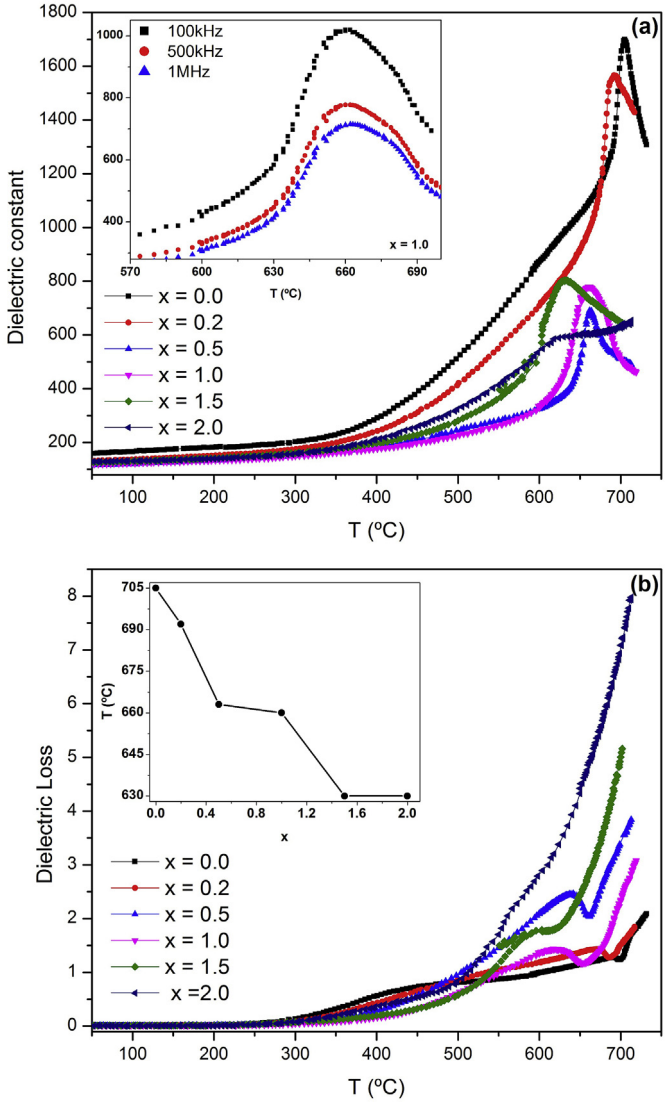

Fig. 5. Temperature dependence of the dielectric constant (a) and loss tangent (b). The data were taken at 500 KHz during the heating process of the thermal cycle. The peak position is frequency independent (inset figure a). The inset in figure b shows the variation of transition temperature (T_c) with x.

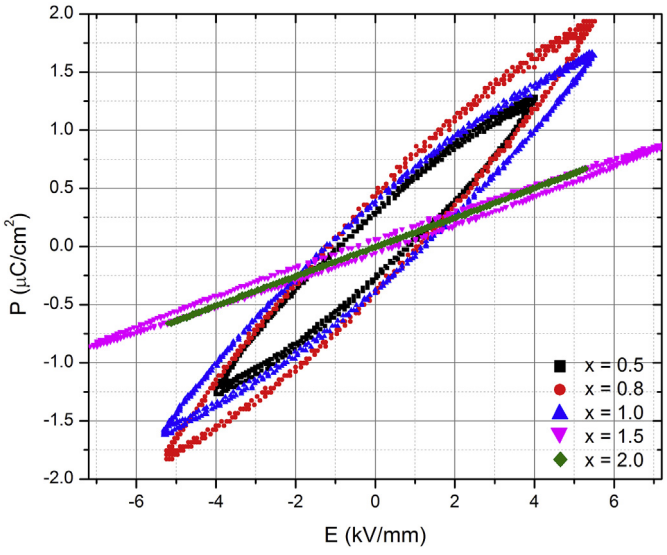

Fig. 6. Polarization hysteresis loops of BTFNx (x = 0.5, 0.8, 1.0, 1.5 and 2.0) ceramics. The cycles were measured at 50 Hz.

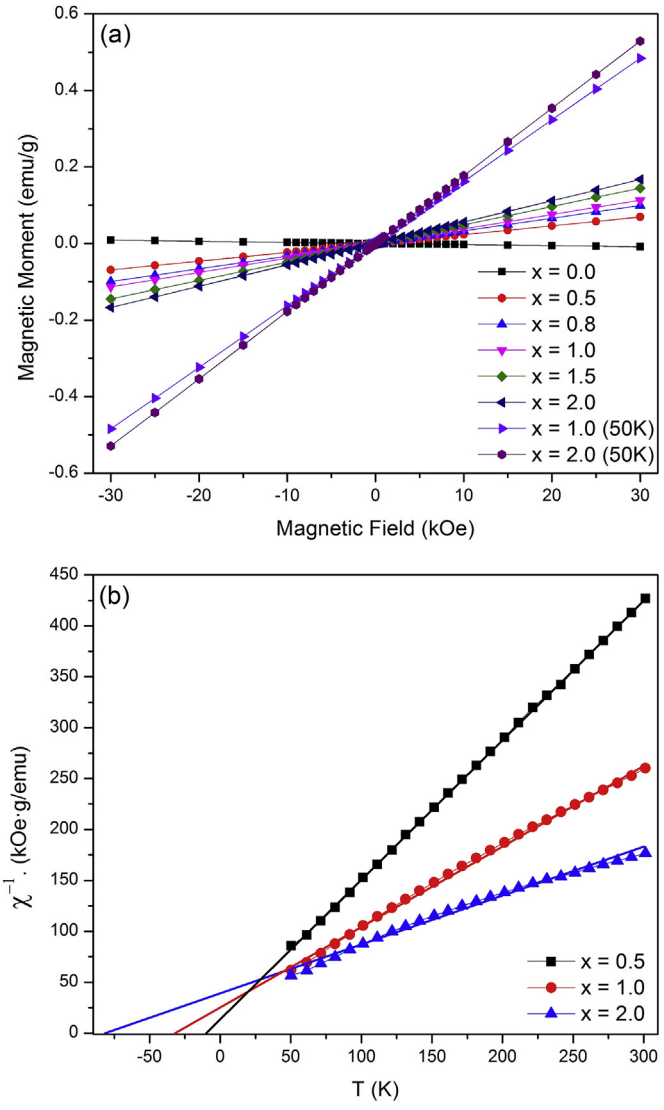

Fig. 7. (a) Field dependences of the magnetization obtained for BTFNx (x = 0.5, 0.8, 1.0, 1.5 and 2.0) ceramic samples at room temperature and T = 50 K (x = 1.0 and 2.0). (b) Temperature dependences of the reciprocal molar magnetic susceptibility measured for BTFNx (x = 0.5, 1.0, and 2.0) ceramics and their Curie–Weiss law fittings.

ions. A secondary pyrochlore phase was detected for x > 1, and this phase is dominant at x = 2.0.

Acknowledgments

We thank Augusto Roman and Laura Steren for their cooperation in the magnetic measurements. We also thank Pablo Diaz and Pablo Botta for the SEM and Raman measurements, respectively. This work was sponsored by Consejo Nacional de Investigaciones Científicas y Tecnológicas (CONICET) and Agencia Nacional de Promoción Científica y Tecnológica (ANPCyT) *de la República Argentina*. MGS thanks support from Consejo de Investigaciones de la Universidad Nacional de Rosario (CIUNR).

References

[1] B.H. Park, B.S. Kang, S.D. Bu, T.W. Noh, J. Lee, W. Jo, Lanthanum-substituted bismuth titanate for use in non-volatile memories, Nature 401 (1999) 682–684.
[2] J.F. Scott, Ferroelectric Memories, Springer Press, Berlin, 2000.

[3] T. Jardiel, A.C. Caballero, M. Villegas, Review: Aurivillius ceramics $Bi_4Ti_3O_{12}$ based piezoelectrics, J. Ceram. Soc. Jpn. 116 (2008) 511–518.
[4] X.Q. Chen, F.J. Yang, W.Q. Cao, D.Y. Wang, K. Chen, Room temperature magnetoelectric coupling in $Bi_4(Ti_1Fe_2)O_{12-\delta}$ system, J. Phys. D: Appl. Phys. 43 (2010) 065001.
[5] X.Q. Chen, F.J. Yang, W.Q. Cao, H. Wang, C.P. Yang, D.Y. Wang, K. Chen, Enhanced multiferroic characteristics in Fe-doped $Bi_4Ti_3O_{12}$ ceramics, Solid State Commun. 150 (2010) 1221–1224.
[6] J. Paul, S. Bhardwaj, K.K. Sharma, R.K. Kotnala, R. Kumar, Room temperature multiferroic behavior and magnetoelectric coupling in Sm/Fe modified $Bi_4Ti_3O_{12}$ ceramics synthesized by solid state reaction method, J. Alloys Compd. 634 (2015) 58–64.
[7] Joginder Paul, Sumit Bhardwaj, K.K. Sharma, R.K. Kotnala, Ravi Kumar, Room temperature multiferroic properties and magnetoelectric coupling in Sm and Ni substituted $Bi_{4-x}Sm_xTi_{3-x}Ni_xO_{12-\delta}$ ($x = 0, 0.02, 0.05, 0.07$) ceramics, J. Appl. Phys. 115 (2014) 204909.
[8] J. Paul, S. Bhardwaj, K.K. Sharma, R.K. Kotnala, R. Kumar, Room temperature multiferroic properties and magnetoelectric coupling in $Bi_{4-x}Sm_xTi_{3-x}Co_xO_{12-\delta}$ in ceramics, J. Mater. Sci. 49 (2014) 6056–6066.
[9] V.A. Khomchenko, G.N. Kakazei, Y.G. Pogorelov, J.P. Araujo, M.V. Bushinsky, D.A. Kiselev, A.L. Kholkin, J.A. Paixão, Effect of Gd substitution on ferroelectric and magnetic properties of $Bi_4Ti_3O_{12}$, Mater. Lett. 64 (2010) 1066–1068.
[10] D.A. Sanchez, N. Ortega, A. Kumar, R. Roque-Malherbe, R. Polanco, J.F. Scott, R.S. Katiyar, Symmetries and multiferroic properties of novel room-temperature magnetoelectrics: lead iron tantalate – lead zirconate titanate (PFT/PZT), AIP Adv. 1 (2011) 042169.
[11] D.M. Evans, A. Schilling, A. Kumar, D. Sanchez, N. Ortega, M. Arredondo, R.S. Katiyar, J.M. Gregg, J.F. Scott, Magnetic switching of ferroelectric domains at room temperature in multiferroic PZTFT, Nat. Commun. 4 (2013) 1534.
[12] D.A. Sanchez, N. Ortega, A. Kumar, G. Sreenivasulu, R.S. Katiyar, J.F. Scott, D.M. Evans, M. Arredondo-Arechavala, A. Schilling, J.M. Gregg, Room-temperature single phase multiferroic magnetoelectrics: $Pb(Fe,M)_x(Zr,Ti)_{(1-x)}O_3$ [M=Ta, Nb], J. Appl. Phys. 113 (2013) 074105.
[13] J. Schiemer, M.A. Carpenter, D.M. Evans, J.M. Gregg, A. Schilling, M. Arredondo, M. Alexe, D. Sanchez, N. Ortega, R.S. Katiyar, M. Echizen, E. Colliver, S. Dutton, J.F. Scott, Studies of the room-temperature multiferroic $Pb(Fe_{0.5}Ta_{0.5})_{0.4}(Zr_{0.53}Ti_{0.47})_{0.6}O_3$: resonant ultrasound spectroscopy, dielectric, and magnetic phenomena, Adv. Funct. Mater. 24 (2014) 2993–3002.
[14] J. Roberto Esquivel-Elizondo, Beverly Brooks Hinojosa, Juan C. Nino, $Bi_2Ti_2O_7$: it is not what you have read, Chem. Mater. 23 (2011) 4965–4974.
[15] I.V. Piir, M.S. Koroleva, Yu.I. Ryabkov, D.A. Korolev, N.V. Chezhina, V.G. Semenov, V.V. Panchuk, Bismuth iron titanate pyrochlores: thermostability, structure and properties, J. Solid State Chem. 204 (2013) 245–250.
[16] L.A.J. Garvie, H. Xu, Y. Wang, R.L. Putnam, Synthesis of $(Ca,Ce^{3+},Ce^{4+})_2Ti_2O_7$: a pyroclore with mixed-valence cerium, J. Phys. Chem. Solids 66 (2005) 902–905.
[17] S. Kojima, S. Shimada, Soft mode spectroscopy of bismuth titanate single crystals, Physica B 219 (1996) 617–619.
[18] L.W. Fu, H. Wang, S.X. Shang, X.L. Wang, P.M. Xu, Preparation and characterization of $Bi_2Ti_2O_7$ thin films grown by metalorganic chemical vapor deposition, J. Cryst. Growth 139 (1994) 319–322.
[19] Fida Rehman, Jing-Bo Li, Mao-Sheng Cao, Yong-Jie Zhao, Muhammad Rizwan, Hai-Bo Jin, Contribution of grains and grain boundaries to dielectric relaxations and conduction of Aurivillius $Bi_4Ti_2Fe_{0.5}Nb_{0.5}O_{12}$ ceramics, Ceram. Int. 41 (2015) 14652–14659.
[20] Wei-Fang Su, Yen-Ting Lu, Synthesis, phase transformation and dielectric properties of sol–gel derived $Bi_2Ti_2O_7$ ceramics, Mater. Chem. Phys. 80 (2003) 632–637.
[21] J. Coey, A. Douvalis, C. Fitzgerald, M. Venkatesan, Ferromagnetism in Fe-doped SnO_2 thin films, Appl. Phys. Lett. 84 (2004) 1332.
[22] H. Meštric, R.A. Eichel, T. Kloss, K.P. Dinse, S. Lanbach, P.C. Schmidt, K.A. Schönau, M. Knapp, H. Ehrenberg, Iron-oxygen vacancy defect centers in $PbTiO_3$: newman superposition model analysis and density functional calculations, Phys. Rev. B 71 (2005) 134109.
[23] A.Y. Birenbaum, C. Ederer, Potentially multiferroic Aurivillius phase $Bi_5FeTi_3O_{15}$: cation site preference, electric polarization, and magnetic coupling from first principles, Phys. Rev. B 90 (2014) 214109.